

ARTICLE

Open Access

Upregulation of LINC01426 promotes the progression and stemness in lung adenocarcinoma by enhancing the level of SHH protein to activate the hedgehog pathway

Xiaoli Liu¹, Zuwei Yin², Linping Xu¹, Huaimin Liu¹, Lifeng Jiang¹, Shuochuan Liu³ and Xu Sun¹

Abstract

Long noncoding RNAs (lncRNAs) play crucial roles in regulating a variety of biological processes in lung adenocarcinoma (LUAD). In our study, we mainly explored the functional roles of a novel lncRNA long intergenic non-protein coding RNA 1426 (LINC01426) in LUAD. We applied bioinformatics analysis to find the expression of LINC01426 was upregulated in LUAD tissue. Functionally, silencing of LINC01426 obviously suppressed the proliferation, migration, epithelial–mesenchymal transition (EMT), and stemness of LUAD cells. Then, we observed that LINC01426 functioned through the hedgehog pathway in LUAD. The effect of LINC01426 knockdown could be fully reversed by adding hedgehog pathway activator SAG. In addition, we proved that LINC01426 could not affect SHH transcription and its mRNA level. Pull-down sliver staining and RIP assay revealed that LINC01426 could interact with USP22. Ubiquitination assays manifested that LINC01426 and USP22 modulated SHH ubiquitination levels. Rescue assays verified that SHH overexpression rescued the cell growth, migration, and stemness suppressed by LINC01426 silencing. In conclusion, LINC01426 promotes LUAD progression by recruiting USP22 to stabilize SHH protein and thus activate the hedgehog pathway.

Introduction

Lung adenocarcinoma (LUAD) is a subtype of non-small cell lung cancer (NSCLC), which has become the most common cancer of tumor-related deaths all over the world^{1–3}. Metastasis occurs in most of the LUAD patients at advanced stage⁴. Although advances have been made in the diagnosis and therapy, the prognosis and overall survival of LUAD patients remain unoptimistic⁵. Thus it is urgent to explore potential molecular mechanisms underlying LUAD progression to find novel therapeutic targets for LUAD patients.

Long noncoding RNAs (lncRNAs) are characterized as a class of transcripts with lengths of more than 200 nucleotides and without protein-coding ability^{6,7}. Accumulating evidence has indicated that lncRNAs are involved in the regulation of various cellular processes. For example, lncRNA NEAT1 acts as a miR-196a-5p sponge to promote colorectal cancer cell proliferation and migration⁸. lncRNA B3GALT5-AS1 inhibits colon cancer metastasis via targeting miR-203⁹. lncRNA EWSAT1 acts as a sponge of miR-326/-330-5p to increase human nasopharyngeal carcinoma cell growth¹⁰. Recent reports have displayed that numerous lncRNAs, including lncRNA DGCR5¹¹, lncRNA HOXA11-AS¹², and lncRNA NEAT1¹³ are associated with LUAD. Here, we investigated the molecular mechanism of a novel lncRNA long intergenic nonprotein coding RNA 1426 (LINC01426) in LUAD. LINC01426 has been reported to be a tumor

Correspondence: Huaimin Liu (lhm1970311@126.com)

¹Affiliated Cancer Hospital of Zhengzhou University & Henan Cancer Hospital, Zhengzhou, China

²Tsinghua University, Beijing, China

Full list of author information is available at the end of the article

Edited by F. Pentimalli

© The Author(s) 2021



Open Access This article is licensed under a Creative Commons Attribution 4.0 International License, which permits use, sharing, adaptation, distribution and reproduction in any medium or format, as long as you give appropriate credit to the original author(s) and the source, provide a link to the Creative Commons license, and indicate if changes were made. The images or other third party material in this article are included in the article's Creative Commons license, unless indicated otherwise in a credit line to the material. If material is not included in the article's Creative Commons license and your intended use is not permitted by statutory regulation or exceeds the permitted use, you will need to obtain permission directly from the copyright holder. To view a copy of this license, visit <http://creativecommons.org/licenses/by/4.0/>.

promoter in glioma¹⁴ and differentially expressed in squamous cell lung carcinoma¹⁵. However, it is unknown whether LINC01426 exerts the same functions in LUAD. Therefore, we investigated its functions in LUAD.

It has been reported that lncRNAs function through multiple pathways, including IGF pathway¹⁶, hedgehog pathway¹⁷, ERK pathway¹⁸, and AKT pathway¹⁹. In our study, we explored the downstream signaling pathway of LINC01426 in LUAD cells.

SHH is a type of protein in the hedgehog pathway and has been reported to take part in the progression of disease²⁰. In our study, we detected the relationship between LINC01426 and SHH in LUAD cells.

As reported previously, USP22 promotes the proliferation of non-small cell lung cancer by regulating the ubiquitination of COX-2²¹. USP22 also regulates EGFR ubiquitination in lung adenocarcinoma²². GSK3 β promotes glioblastoma tumorigenesis through inducing KDM1A deubiquitination by USP22²³. In our study, we also investigated whether USP22 was involved in the LINC01426-mediated hedgehog pathway.

Taken together, we aimed at exploring the functions of LINC01426 in LUAD and its regulatory mechanism with the hedgehog pathway.

Materials and methods

Cell lines and reagents

Human bronchial epithelial cell line (HBE) and human LUAD cell lines (H1299, A549, PC-9, Calu3) used in this study were procured from ATCC (Manassas, VA). They were grown with 10% FBS and 1% antibiotics in DMEM (Invitrogen, Carlsbad, CA) under 37 °C and 5% CO₂. To treat PC-9 and Calu3 cells, 5 μ g/ml of cycloheximide (CHX), 20 mmol/l of LiCl were available from Sigma-Aldrich (St. Louis, MO). A total of 20 mg/ml of MG132 and 100 μ M of NSC 228155, 50 μ M of Honokiol were purchased from Selleck Chemicals (Houston, TX). Totally, 10 nM of IGF-1 was bought from PeprTech (Rocky Hill, NJ). Totally, 10 nM of SAG was obtained from Abcam (Cambridge, MA).

Total RNA isolation and qRT-PCR

Total RNA isolation from cultured cells was complete using Trizol reagent (Invitrogen), then cDNA was synthesized by PrimeScript™ RT reagent kit as guided (Takara, Shiga, Japan). Gene expression was evaluated by qRT-PCR with SYBR Premix Ex Taq II (Takara) and calculated based on the 2^{- $\Delta\Delta$ Ct} method. GAPDH or U6 served as the reference gene.

Subcellular fractionation assay

1 \times 10⁶ PC-9 and Calu3 cells were collected, then centrifuged and washed in phosphate-buffered saline (PBS). PARIS™ was applied to perform subcellular fractionation

assay as required (Invitrogen). LINC01426 content was examined in the cell cytoplasm and cell nucleus with qRT-PCR.

Fluorescence in situ hybridization

Cells fixed by 4% formaldehyde were rinsed in PBS and digested, then dehydrated and hybridized with LINC01426-FISH probe (Ribobio, Guangzhou, China). The cell nucleus was counterstained by DAPI solution and visualized by fluorescence microscope (Olympus Corp., Tokyo, Japan).

Transfection

The short hairpin RNAs (shRNAs) specifically targeting LINC01426 or USP22 were synthesized by GenePharma (Shanghai, China) and transfected into cancer cells using Lipofectamine 2000 (Invitrogen). The full-length cDNA sequence of SHH was inserted into the pcDNA3.1 vector (Invitrogen) for overexpression. All transfections were conducted for 48 h.

Colony formation assay

PC-9 and Calu3 cells were cultured for 14 days in 6-well plates at a density of 500/well. After that, cells were fixed in 4% paraformaldehyde, stained with 0.1% crystal violet, and finally counted manually.

EdU staining

Cells were seeded in 96-well plates at 5 \times 10⁴ density for incubation with EdU medium diluent and fixed for 2 h. Cell proliferation was assayed based on the protocol of the EdU staining reagent (Ribobio). After washing in PBS, cells were cultured in DAPI solution, then observed under a fluorescence microscope.

Flow cytometry analysis

The transfected cells (2 \times 10⁵) were harvested and rinsed in precooled PBS, then treated with Annexin V-FITC/PI Apoptosis kit as per user manual (BD Biosciences, San Jose, CA). After double-staining in binding buffer, a flow cytometer was used based on the protocol (BD Biosciences).

TUNEL staining

Terminal deoxynucleotidyl transferase dUTP nick end labeling (TUNEL) staining reagent was available from Beyotime (Haimen, China) to detect apoptotic cells. After fixing and washing, cells were permeabilized in 0.1% TritonX-100 for staining with TUNEL kit and DAPI solution, then examined using a fluorescence microscope.

JC-1 staining

After 5 min of centrifugation, the processed cells in 96-well plates were treated with JC-1 staining reagent

(Beyotime) for 30 min. Following washing in assay buffer, mitochondrial transmembrane potential ($\Delta\Psi_m$) was monitored by a fluorescent plate reader.

Transwell migration assay

Migration assay was completed using the Transwell chamber (8-mm pore size; Corning, Corning, NY). The lower chamber was filled with 100% medium, and cells re-suspended in serum-free medium were seeded in the upper chamber for 24 h. Then, cells migrated to the bottom surface were fixed and stained by crystal violet dye. Five fields were randomly selected for counting with a microscope.

Western blot

Total protein samples were isolated using radio-immunoprecipitation assay lysis buffer and separated on 12% sodium dodecyl sulfate-polyacrylamide gel electrophoresis, then transferred to polyvinylidene fluoride membranes and cultured with 5% nonfat milk. After that, the primary antibodies against N-cadherin, E-cadherin, NANOG, OCT4, SHH, DHH, IHH, Gli1, Gli2, USP22, and GAPDH (internal reference), as well as secondary antibodies labeled by horseradish peroxidase, were all procured from Abcam (Cambridge, MA) and used to incubate membranes. Signals of protein bands were detected using an ECL system (Bio-Rad, Hercules, CA).

Immunofluorescence staining (IF)

Cells were cultured for 24 h on culture slides and washed in PBS after adhering to slides. Then, the fixed cells were treated with 5% bovine serum albumin and incubated with primary antibodies specific to E-cadherin and N-cadherin. Following washing, secondary antibody was added, the slides were stained in DAPI and examined by Olympus microscope.

Sphere formation assay

Cell lines were cultured with sphere medium in the 96-well ultralow attachment plates in line with instruction (Corning) for 7 days, with 10 cells in each well. Cell clusters with a diameter >50 μ m were seen as sphere cells and counted.

Co-immunoprecipitation (Co-IP)

Cells were treated with IP lysis buffer, then lysates were probed with SHH or USP22 antibody and magnetic beads at 4 °C all night. After that, samples were washed in PBS and eluted for western blot.

RNA pull-down assay

Pierce Magnetic RNA-Protein Pull-Down Kit was available from Thermo Fisher Scientific (Waltham, MA) and used as instructed. Cell lysates were mixed with

biotinylated RNA probes for LINC01426 and its antisense RNA (LINC01426 AS), then added with magnetic beads for 1 h. After elution, a western blot assay was performed to detect the recovered proteins.

RNA immunoprecipitation (RIP) assay

After culturing in RIP lysis buffer, lysates from processed cells were conjugated with USP22 antibody or control IgG antibody in magnetic beads. After RNA enrichment, qRT-PCR was implemented to analyze RNA enrichment.

Tumor xenograft

The Animal Research Committee of Affiliated Cancer Hospital of Zhengzhou University approved the protocols for animal experiments. The mice (4-week-old BALB/c nude female mice, 5 per group) were subcutaneously injected with PC-9 cells stably transfected with sh/Ctrl, sh/LINC01426#1, and sh/LINC01426#1+SHH, and every four days the tumor volume was recorded. The mice were all sacrificed on the 28th day and tumor tissues were collected to measure tumor weight.

Statistical analysis

The experiments in our study were all conducted in triplicate, results were given as the means \pm standard deviation (S.D.) and analyzed using PRISM 6 as guided (GraphPad, San Diego, CA). The statistical analysis was performed using Student's *t* test or one-way (two-way) ANOVA. The significant level was set as p-values below 0.05.

Results

LINC01426 is overexpressed in LUAD

At first, we searched on the GEPIA database (<http://gepia2.cancer-pku.cn/#analysis>) and found that LINC01426 was expressed at a high level in 483 LUAD tissues compared to 347 normal tissues (Fig. 1A). In addition, we used RT-qPCR to confirm that LINC01426 expression was evidently increased in LUAD cell lines (H1299, A549, PC-9, and Calu3) compared to HBE cell line HBE (Fig. 1B). We selected PC-9 and Calu3 cells for subsequent experiments due to the expression of LINC01426 was expressed highest in these two cells. Furthermore, the Subcellular fractionation assay and FISH assays analyzed that LINC01426 was mainly distributed in the cytoplasm (Fig. 1C, D). Taken together, LINC01426 is highly expressed in LUAD samples and cells.

Silencing of LINC01426 inhibits proliferation and promotes apoptosis of LUAD cells

LINC01426 expression was silenced in PC-9 and Calu3 cells to explore the functions of LINC01426 in LUAD cells (Fig. 2A). It was revealed that the proliferation of

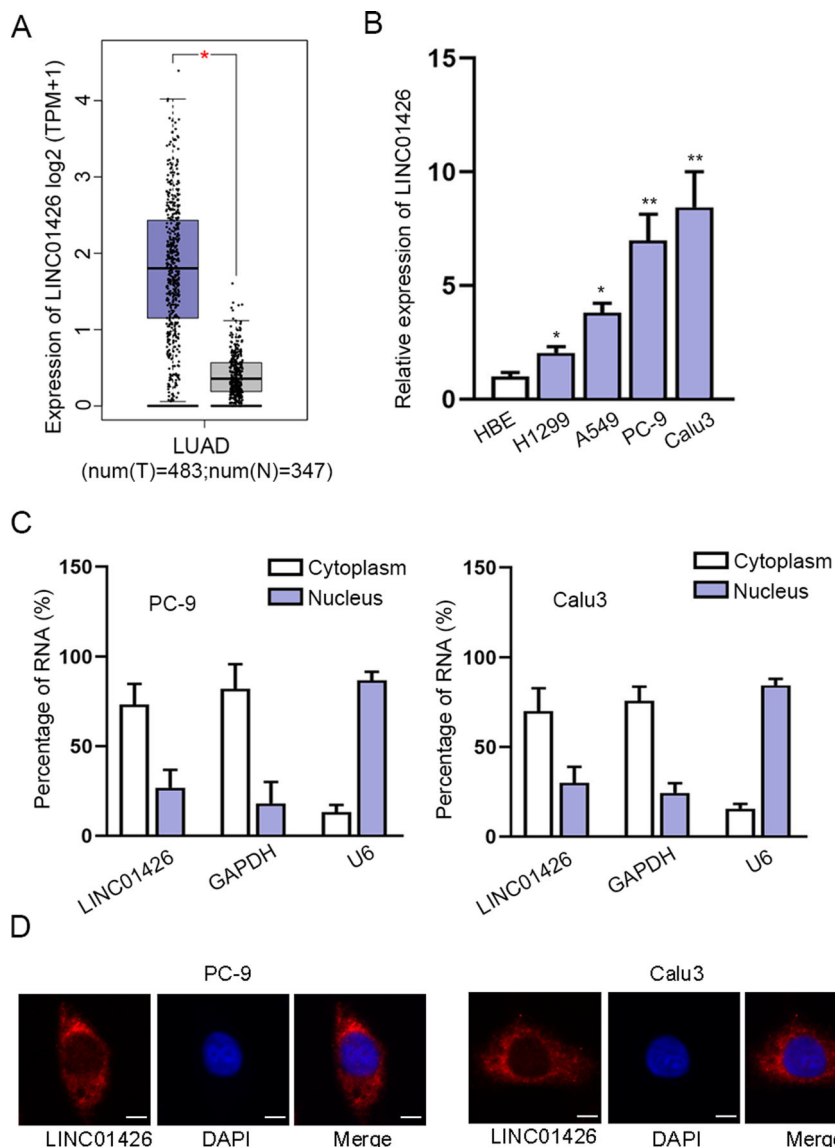


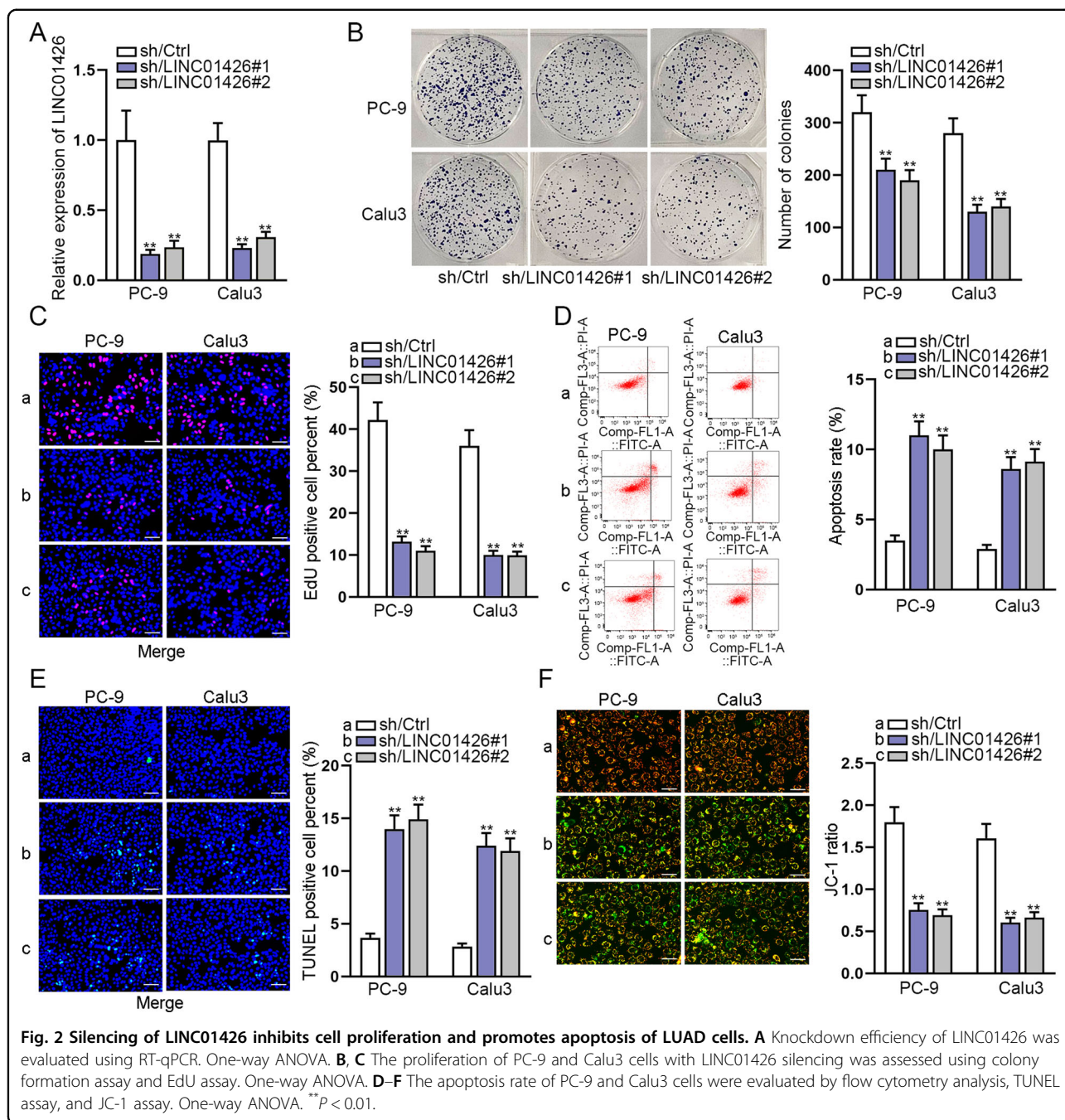
Fig. 1 LINC01426 is overexpressed in LUAD. **A** LINC01426 expression in LUAD tissues (left panel; $n = 483$) and normal tissues (right panel; $n = 347$) based on the GEPIA2 database. Unpaired Student's t test. **B** The relative level of LINC01426 in LUAD cells was measured using RT-qPCR. One-way ANOVA. **C, D** Subcellular fractionation assay and FISH assay analyzed the cellular location of LINC01426. * $P < 0.05$, ** $P < 0.01$.

PC-9 and Calu3 cells was drastically inhibited by LINC01426 knockdown through colony formation and EdU assays (Fig. 2B, C). Moreover, flow cytometry analysis, TUNEL assay, and JC-1 assay demonstrated that the apoptosis rate of PC-9 and Calu3 cells were increased by LINC01426 knockdown (Fig. 2D–F). All these results showed that silencing of LINC01426 inhibits LUAD cell growth.

LINC01426 knockdown suppresses migration, EMT, and stemness of LUAD cells

We further determine whether LINC01426 could regulate other cell functions in LUAD. Transwell assay certified that LINC01426 knockdown suppressed the

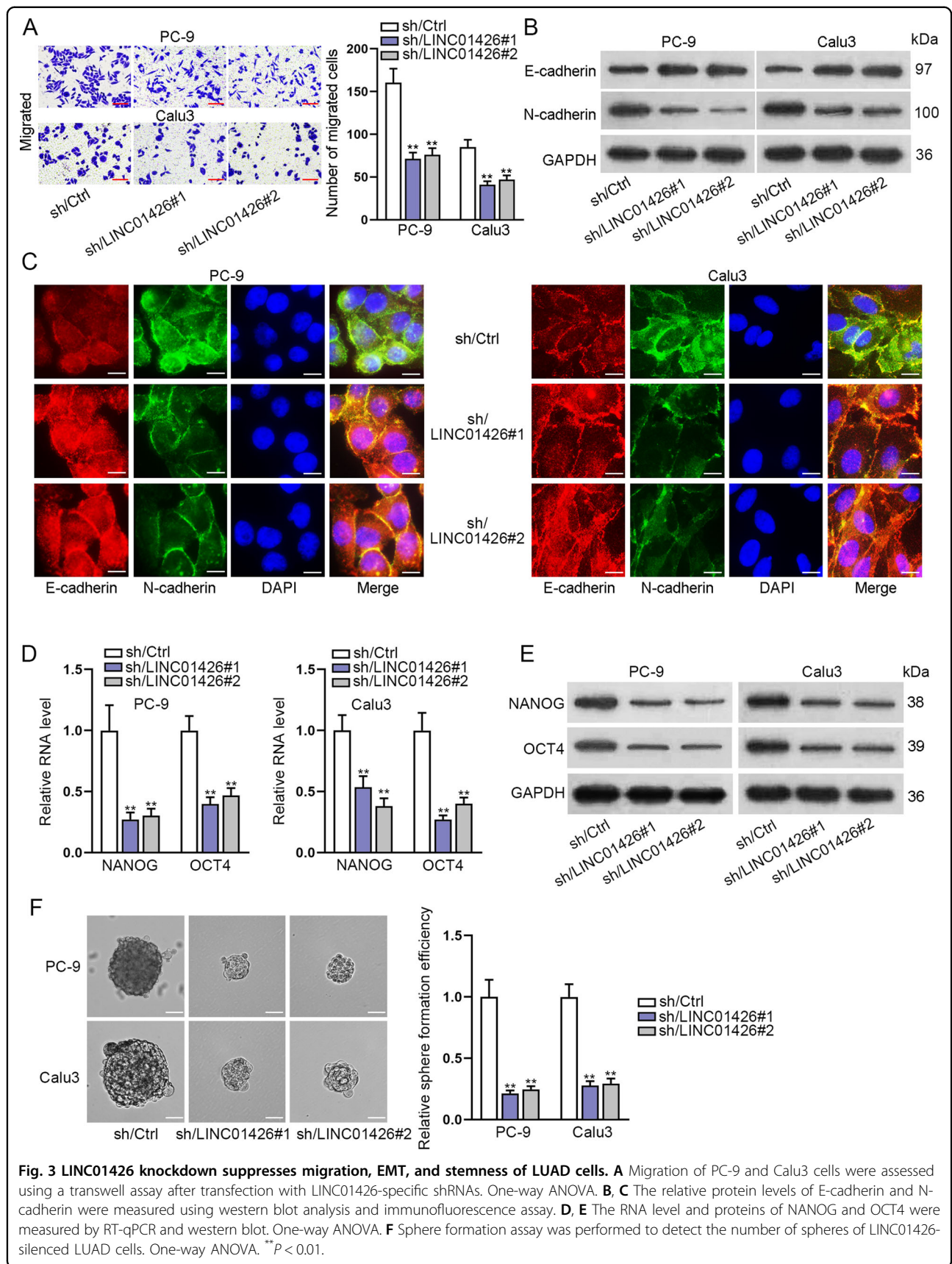
migration of PC-9 and Calu3 cells (Fig. 3A). Western blot analysis and IF assays revealed that LINC01426 knockdown increased the expression of E-cadherin while decreased N-cadherin expression in LUAD cells (Fig. 3B, C). Furthermore, the mRNA and protein levels of NANOG and OCT4 (stemness markers) were reduced by LINC01426 knockdown in PC-9 and Calu3 cells (Fig. 3D, E). Sphere formation assay further certified that LINC01426 knockdown suppressed the sphere formation capacity of PC-9 and Calu3 cells (Fig. 3F). All these results indicated that LINC01426 knockdown suppresses the migration, EMT, and stemness of LUAD cells.



LINC01426 promotes LUAD progression by activating the hedgehog pathway

LncRNAs have been reported to function in LUAD through various signaling pathways. Here, we added activators of these pathways into PC-9 and Calu3 cells transfected with sh/LINC01426#1 to observe the changes in colony formation ability. The results indicated that the number of colonies reduced by LINC01426 silencing was apparently increased by the treatment SAG activator

(Fig. 4A), indicating that LINC01426 functioned in LUAD cells potentially through activating the hedgehog pathway. EdU assay further proved that SAG could completely rescue the EdU positive cells of LINC01426 knockdown in PC-9 and Calu3 cells (Fig. 4B). It was shown that the apoptosis rate enhanced by LINC01426 downregulation was decreased again by SAG (Fig. 4C, D). Furthermore, a transwell assay was performed to disclose that silencing of LINC01426 depleted the migration of PC-9 and Calu3



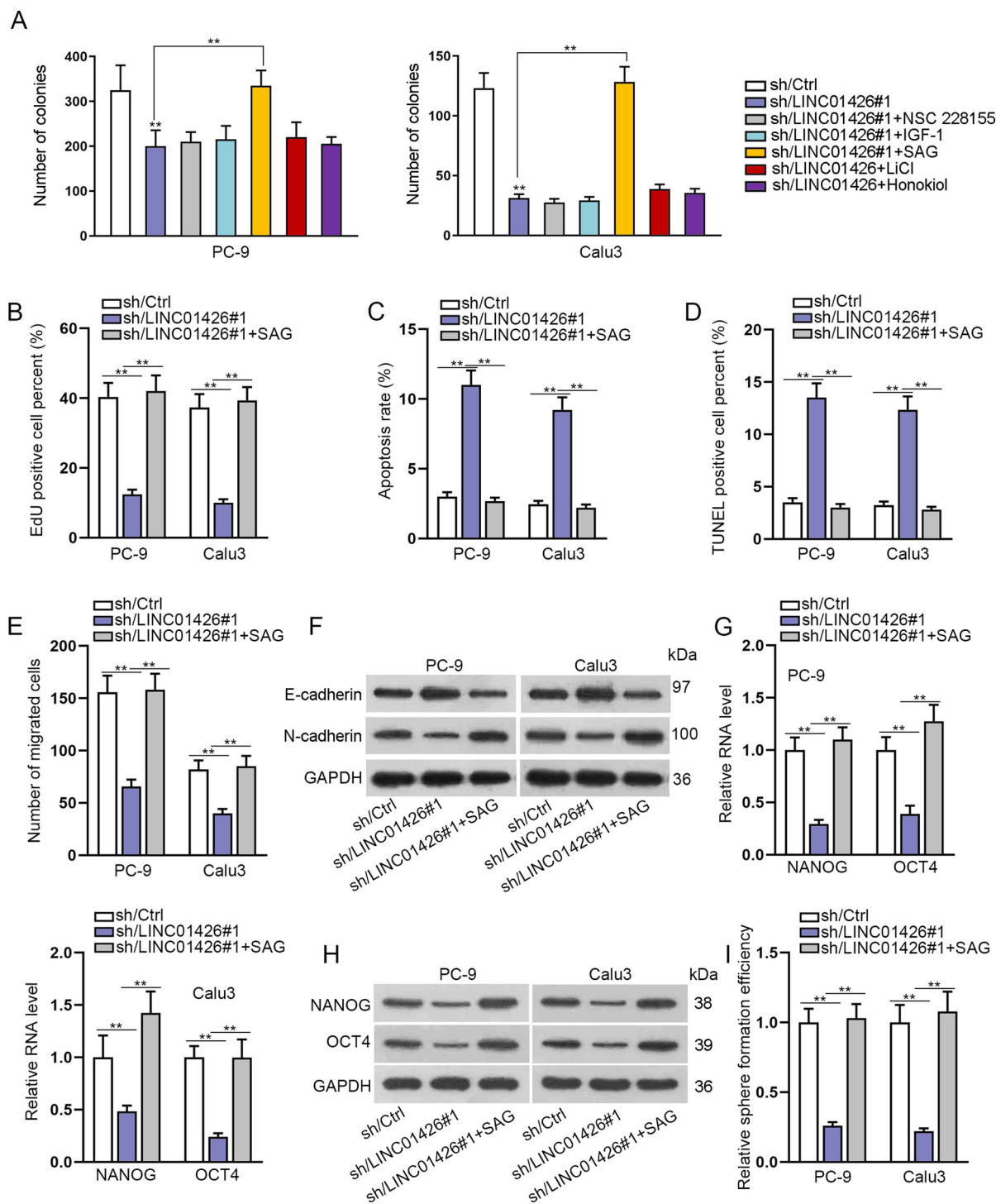
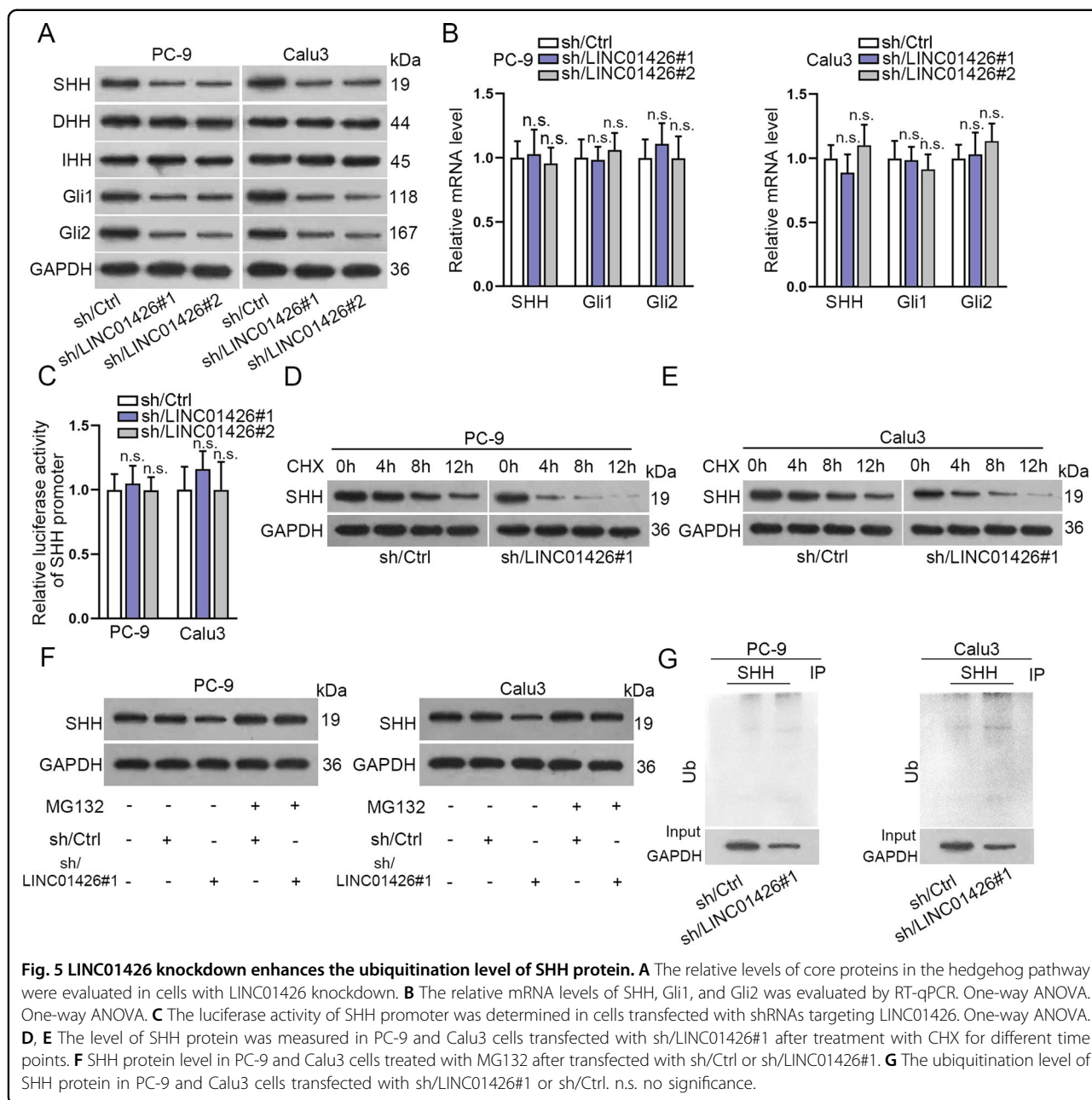


Fig. 4 LINC01426 promotes LUAD progression through activating the hedgehog pathway. **A** The number of colonies was analyzed in PC-9 and Calu3 cells treated with sh/Ctrl, sh/LINC01426#1, sh/LINC01426#1+NSC 228155, sh/LINC01426#1+IGF-1, sh/LINC01426#1+SAG, sh/LINC01426#1+LiCl, sh/LINC01426#1+Honokiol, respectively. One-way ANOVA. PC-9 and Calu3 cells were treated with sh/Ctrl, sh/LINC01426#1, or sh/LINC01426#1+SAG and used for subsequent rescue experiments. **B** EdU-positive cells were assessed by EdU assay. One-way ANOVA. **C, D** The apoptosis rate was evaluated by flow cytometry analysis and TUNEL assay. One-way ANOVA. **E** The migratory capacity was tested by transwell assay. One-way ANOVA. **F** The relative protein levels of E-cadherin and N-cadherin were detected by western blot. One-way ANOVA. **G, H** The RNA and protein levels of NANOG and OCT4 were examined by RT-qPCR and western blot in indicated cells. One-way ANOVA. **I** Sphere formation assay was conducted to test the efficiency of the sphere in indicated cells. One-way ANOVA. ***P* < 0.01.



cells, whereas this effect could be reversed by the treatment of SAG (Fig. 4E). In addition, the increased protein level of E-cadherin and the decreased protein level of N-cadherin caused by LINC01426 silencing were recovered after SAG treatment (Fig. 4F). RT-qPCR and western blot analyzed that the expression of NANOG and OCT4 lessened by LINC01426 knockdown was strengthened by SAG treatment (Fig. 4G, H). Sphere formation assay further asserted that the sphere formation ability of LUAD cells reduced by LINC01426 knockdown was enhanced by SAG treatment (Fig. 4I). In short, LINC01426 exerts functions in LUAD through the hedgehog pathway.

LINC01426 knockdown enhances the ubiquitination level of SHH protein

We further used western blot to analyze the expression of the relative proteins in the hedgehog pathway. As shown in Fig. 5A, the expression of SHH, Gli1, and Gli2 were distinctly reduced by LINC01426 knockdown, while no significant difference between DHH and IHH in PC-9 and Calu3 cells. RT-qPCR examined that the expression of SHH, Gli1, and Gli2 was not changed by LINC01426 knockdown in PC-9 and Calu3 cells (Fig. 5B). Luciferase reporter assay further proved that the luciferase activity of SHH promoter was not changed in PC-9 and Calu3 cells

transfected with shRNAs targeting LINC01426 (Fig. 5C), suggesting that LINC01426 could not affect the transcription of SHH. Therefore, we further investigated whether LINC01426 regulated SHH protein. We treated LINC01426-silenced PC-9 and Calu3 cells with CHX to test SHH protein level. Compared with the control group, the half-life of SHH was much shorter in LINC01426-silenced PC-9 and Calu3 cells than that in control cells (Fig. 5D, E and Fig. S1A). SHH protein level was also detected in PC-9 and Calu3 cells transfected with sh/Ctrl or sh/LINC01426#1 treated with or without MG132. It was uncovered that SHH protein level was increased in cells treated with MG132 and this tendency could not be changed by LINC01426 silencing (Fig. 5F). Thus, we hypothesized that LINC01426 might affect SHH protein decay. Ubiquitination experiments further validated that silencing of LINC01426 promoted the ubiquitination of SHH (Fig. 5G). Totally, LINC01426 knockdown regulates the ubiquitination of SHH protein and thus activates the hedgehog pathway.

LINC01426 binds with USP22 to promote SHH deubiquitination

To explore the mechanism by which LINC01426 regulated USP22 protein, pull-down sliver staining was conducted to find potential proteins interacting with LINC01426, and spectrometry analysis confirmed that USP22 was the protein that could closely bind with LINC01426 (Fig. 6A). Pull-down Silver staining followed by western blot analysis further demonstrated the interaction between LINC01426 and USP22 in PC-9 and Calu3 cells (Fig. 6B). RIP assay indicated that LINC01426 was enriched in the anti-USP22 group (Fig. 6C). Through co-IP assay, we determined that the interaction between SHH and USP22 was disrupted by LINC01426 knockdown (Fig. 6D, E and Fig. S1B). According to the correlation analysis of the GEPIA database, there was no significant correlation between LINC01426 and USP22 as well as between USP22 and SHH (Fig. S1C, D). However, LINC01426 and SHH were positively correlated with each other (Fig. S1E). Their interaction was further proven by FISH co-localization analysis (Fig. S1F). Importantly, there no regulatory effect of LINC01426 on USP22 expression (Fig. S1G). Moreover, we silenced in PC-9 and Calu3 cells for further study (Fig. S2A). We applied western blot to demonstrate that the half-life of SHH and USP22 was decreased in PC-9 and Calu3 cells transfected with sh/USP22#1 (Fig. 6F, G and Fig. S2B). Meanwhile, the protein level of SHH enhanced by MG132 was not changed by USP22 silencing (Fig. 6H). Ubiquitination assay revealed that USP22 silencing could promote the ubiquitination level of SHH (Figure S2,C). Ubiquitination assays manifested that downregulation of LINC01426 increased SHH ubiquitination in PC-9 and Calu3 cells supplemented with MG132 (Fig. 6I).

Collectively, LINC01426 can recruit USP22 to promote SHH deubiquitination.

SHH overexpression reverses the inhibitory effect of LINC01426 knockdown on LUAD cell proliferation, migration, EMT, and stemness

To explore the role of SHH in the LUAD cells, we overexpressed SHH in PC-9 cells (Fig. S3A) and conducted rescue assays. It was displayed in colony formation and EdU assays that SHH overexpression reversed the suppressive effect of LINC01426 knockdown on cell proliferation (Fig. 7A, B). Furthermore, the apoptosis rate enhanced by LINC01426 silencing was decreased again after overexpression of SHH (Fig. 7C, D). Transwell assay revealed the number of migrated cells reduced by LINC01426 knockdown was increased again by SHH promotion (Fig. 7E). The effect of LINC01426 down-regulation on EMT-related proteins was attenuated by SHH overexpression (Fig. 7F). Furthermore, the stemness weakened by LINC01426 silencing was strengthened again by the upregulation of SHH of NANOG, and OCT4 was reduced by LINC01426 reduction, and completely overset by overexpressed SHH (Fig. 7G–I).

In vivo experiments were also conducted to validate the role of the LINC01426/SHH axis in LUAD tumor growth. Tumor size, volume, and weight in the sh/LINC01426#1 group were smaller than those in the sh/Ctrl group, whereas, all those indexes were amplified in the sh/LINC01426#1+SHH group (Fig. S3B–D). We also examined the expression level of LINC01426, USP22, and SHH in three groups. It was uncovered that the levels of LINC01426 were decreased in the sh/LINC01426#1 group but were not changed in the sh/LINC01426#1+SHH group. The level of USP22 in the three groups showed no significant difference. However, the level of SHH decreased by LINC01426 silencing was enhanced again after introduction with SHH expression vector (Fig. S3E). IHC assay revealed that the positivity of Ki-67 and PCNA decreased by LINC01426 was enhanced after over-expression of SHH (Fig. S3F).

All these results showed that LINC01426 facilitates LUAD progression via deubiquitination of SHH protein to activate the hedgehog pathway (Fig. 8).

Discussion

Mounting evidence has revealed that lncRNAs play vital roles in the progression of LUAD. For instance, LINC01614 promotes LUAD cell progression by miR-217/FOXP1 axis²⁴. LncRNA CAR10 enhances LUAD metastasis through miR-203/30/SNAI axis²⁵. LncRNA SPRY4-IT1 plays important role in tumor cell migration and invasion of LUAD²⁶. However, the association between LINC01426 and LUAD was uncovered. In our study, the expression of LINC01426 was found to be dramatically

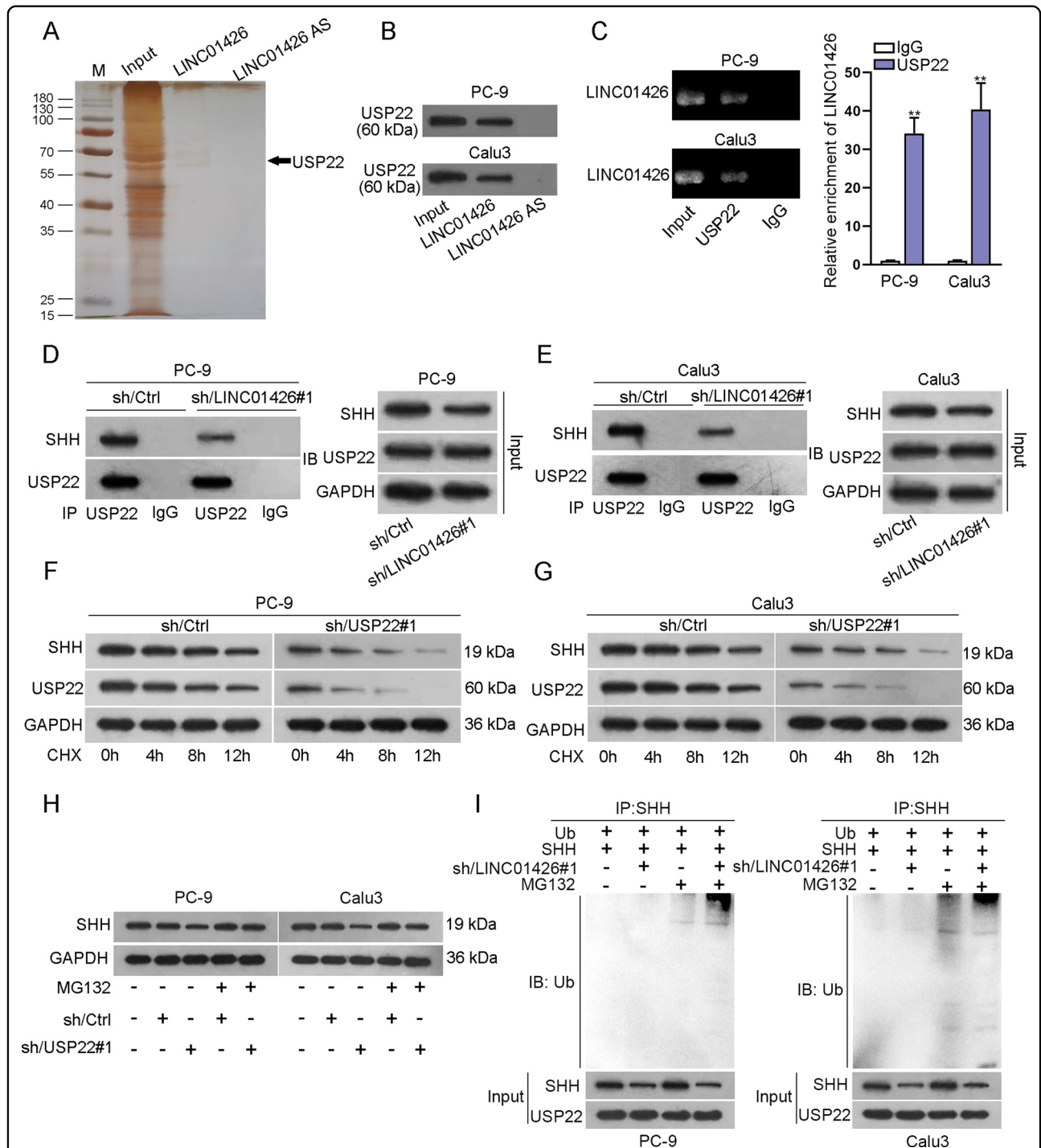


Fig. 6 LINC01426 binds with USP22 to promote SHH deubiquitination. **A** Pull-down sliver staining assay and spectrometry analysis assessed the potential proteins combined with LINC01426. **B** Pull-down and western blot analysis revealed the interaction between USP22 and LINC01426. **C** RIP assay examined the enrichment of LINC01426 in the anti-USP22 group and anti-IgG. One-way ANOVA. **D, E** The binding of SHH and USP22 was disrupted by LINC01426. **F, G.** The level of SHH or USP22 protein was detected in LINC01426-silenced PC-9 and Calu3 cells after treatment with CHX for different time points. **H** SHH protein was detected in USP22-silenced PC-9 and Calu3 cells treated with MG132. **I** Ubiquitination assay was used to detecting SHH ubiquitination in PC-9 and Calu3 cells transfected with sh/LINC01426#1 after treated with MG132. ***P* < 0.01.

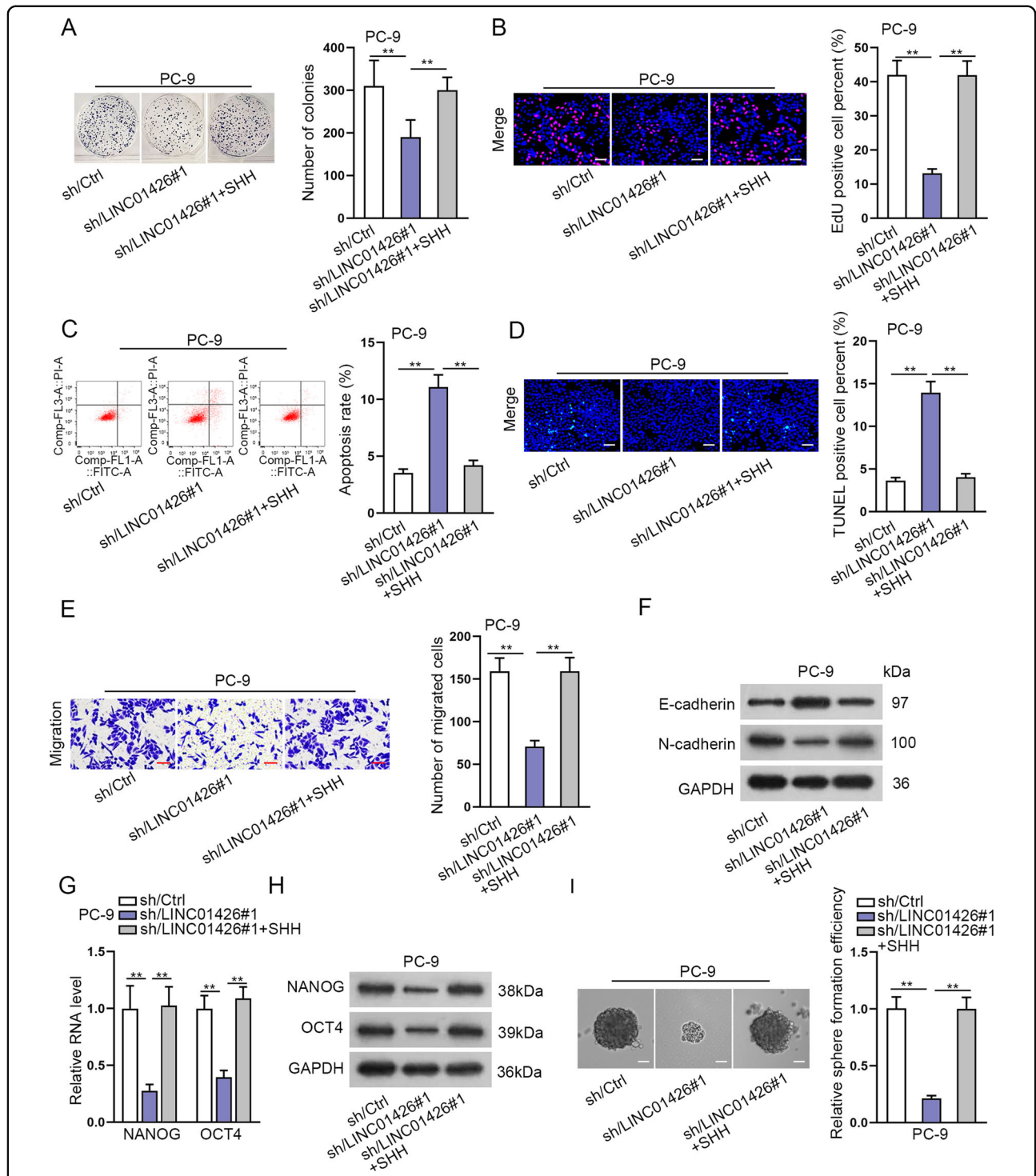


Fig. 7 SHH overexpression reverses the inhibitory effect of LINC01426 knockdown on LUAD cell proliferation, migration, EMT, and stemness. **A, B.** The proliferation in PC-9 cells transfected with sh/LINC01426#1 or sh/LINC01426#1+SHH was measured using colony formation and EdU assays. One-way ANOVA. **C, D** The apoptosis rate was determined in PC-9 cells transfected with sh/Ctrl, sh/LINC01426#1 or sh/LINC01426#1+SHH by flow cytometry analysis and TUNEL assay. One-way ANOVA. **E** The number of migrated cells was determined in PC-9 cells transfected with sh/Ctrl, sh/LINC01426#1, or sh/LINC01426#1+SHH by transwell assay. One-way ANOVA. **F** The protein levels of E-cadherin and N-cadherin were analyzed in PC-9 cells transfected with sh/Ctrl, sh/LINC01426#1, or sh/LINC01426#1+SHH using western blot analysis. One-way ANOVA. **G, H** The relative RNA and protein levels of stemness markers were detected by RT-qPCR and western blot in indicated PC-9 cells. One-way ANOVA. **I** Sphere formation assay detected the number of spheres in PC-9 cells. One-way ANOVA. ***P* < 0.01.

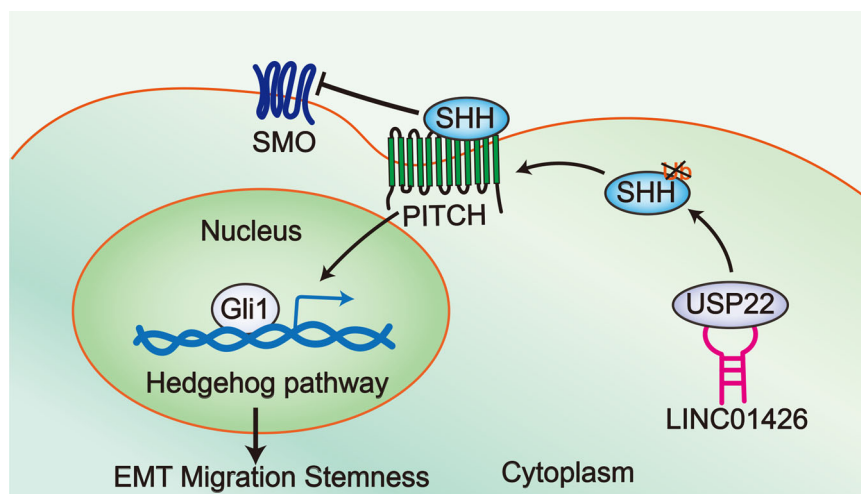


Fig. 8 A scientific diagram was generated to illustrate the role of LINC01426 in modulating the LUAD cellular process through the hedgehog pathway.

upregulated in LUAD cells. Through loss-of-function assays, we found that LINC01426 knockdown suppressed LUAD cell proliferation and migration. Moreover, EMT and stemness were important processes in LUAD development. We found that silencing of LINC01426 also significantly inhibited the EMT and stemness of LUAD cells. Together, our study suggested that LINC01426 might play an oncogenic role in LUAD, which might be an underlying therapeutic target in LUAD.

To explore the mechanism of LINC01426-regulated LUAD cellular processes, our research further studied the potential underlying signaling pathways. Recently, it has been reported that abnormal activation of multiple signaling pathways is important to LUAD progression. For example, LPCAT1 regulates LUAD metastasis by activating PI3K/AKT/MYC pathway²⁷. NRG1 suppresses human lung adenocarcinoma through AKT and ERK1/2 pathway²⁸. FLOT1 affects the progression of lung adenocarcinoma by regulating the Erk/Akt signaling pathway²⁹. In our study, we observed that LINC01426 functioned in LUAD cells through the hedgehog pathway. Hedgehog pathway plays momentous roles in many malignant tumors, such as hepatocellular carcinoma³⁰, medulloblastoma³¹, glioblastoma³², and pancreatic cancer³³. Through further investigation, we found that LINC01426 knockdown inhibited the protein level of SHH but had no significant effect on its mRNA level. Moreover, LINC01406 could not affect SHH transcription. Therefore, we explored whether LINC01426 regulated the stability of SHH protein.

USP22 has been reported to involve in tumorigenesis and progression. For example, MiR-101 impedes the tumorigenesis of papillary thyroid carcinoma by targeting USP22³⁴. MiR-30e-5p targets USP22 to suppress the proliferation of

nasopharyngeal carcinoma cells³⁵. Silencing of USP22 promotes human retinoblastoma cell apoptosis by inhibiting TERT/P53 pathway³⁶. Here, we uncovered that LINC01426 could interact with USP22 in LUAD cells. It has been reported that ubiquitination plays vital roles in a variety of biological processes, including cell survival and differentiation as well as innate and adaptive immunity³⁷. LncRNAs can interact with ubiquitination-related proteins to modulate the protein level of their downstream targets. For instance, lncRNA uc.134 inhibits CUL4A-mediated ubiquitination of LATS1 to hinder hepatocellular carcinoma progression³⁸. LncRNA MEG3 suppresses the progression of gallbladder cancer by promoting the ubiquitination of EZH2 to regulate LATS2³⁹. USP22 is known as a deubiquitinase. Here, we determined that LINC01426 interacted with USP22 to stabilize SHH protein.

In summary, our study demonstrated the role of LINC01426 in LUAD progression. LINC01426 knockdown impeded the progression, migration, EMT, and stemness of LUAD cells. In addition, upregulation of LINC01426 promotes LUAD progression by enhancing the level of SHH protein to activate the hedgehog pathway. Our findings may contribute to LINC01426 may serve as a potential therapeutic target in LUAD. Lacking clinical study is a shortcoming of the current study. We will probe the clinical significance of LINC01426 for LUAD patients.

Acknowledgements

Sincere thanks for the help from the lab members.

Author details

¹Affiliated Cancer Hospital of Zhengzhou University & Henan Cancer Hospital, Zhengzhou, China. ²Tsinghua University, Beijing, China. ³Queen Mary College of Medicine, Nanchang University, Nanchang, China

Author contributions

Xiaoli Liu designed this study and was responsible for article writing. Zuwei Yin, Linping Xu, and Huaimin Liu collected experimental materials and performed experiments. While Lifeng Jiang, Shuochuan Liu, and Xu Sun analyzed the experimental data and prepared all figures. All authors read and approved the final paper.

Ethics statement

The Animal Research Committee of Affiliated Cancer Hospital of Zhengzhou University approved the protocols for animal experiments.

Conflict of interest

The authors declare that they have no conflict of interest.

Publisher's note

Springer Nature remains neutral with regard to jurisdictional claims in published maps and institutional affiliations.

Supplementary information

The online version contains supplementary material available at <https://doi.org/10.1038/s41419-021-03435-y>.

Received: 27 February 2020 Revised: 25 November 2020 Accepted: 18 December 2020

Published online: 10 February 2021

References

- Siegel, R. L., Miller, K. D. & Jemal, A. Cancer Statistics, 2017. *CA Cancer J. Clin.* **67**, 7–30 (2017).
- Hasan, N., Kumar, R. & Kavuru, M. S. Lung cancer screening beyond low-dose computed tomography: the role of novel biomarkers. *Lung* **192**, 639–648 (2014).
- Travis, W. D. The 2015 WHO classification of lung tumors. *Der Pathol.* **35**(Suppl 2), 188 (2014).
- Gridelli, C. et al. Non-small-cell lung cancer. *Nat. Rev. Dis. Prim.* **1**, 15009 (2015).
- Wang, J. et al. BIN1 reverses PD-L1-mediated immune escape by inactivating the c-MYC and EGFR/MAPK signaling pathways in non-small cell lung cancer. *Oncogene* **36**, 6235–6243 (2017).
- Katsushima, K. et al. Targeting the Notch-regulated non-coding RNA TUG1 for glioma treatment. *Nat. Commun.* **7**, 13616 (2016).
- Nagano, T. & Fraser, P. No-nonsense functions for long noncoding RNAs. *Cell* **145**, 178–181 (2011).
- Zhong, F. et al. LncRNA NEAT1 promotes colorectal cancer cell proliferation and migration via regulating glial cell-derived neurotrophic factor by sponging miR-196a-5p. *Acta Biochim. Biophys. Sin.* **50**, 1190–1199 (2018).
- Wang, L. et al. Long noncoding RNA B3GALT5-AS1 suppresses colon cancer liver metastasis via repressing microRNA-203. *Aging* **10**, 3662–3682 (2018).
- Song, P. & Yin, S. C. Long non-coding RNA EWSAT1 promotes human nasopharyngeal carcinoma cell growth in vitro by targeting miR-326/-330-5p. *Aging* **8**, 2948–2960 (2016).
- Dong, H. X., Wang, R., Jin, X. Y., Zeng, J. & Pan, J. LncRNA DGCR5 promotes lung adenocarcinoma (LUAD) progression via inhibiting hsa-mir-22-3p. *J. Cell. Physiol.* **233**, 4126–4136 (2018).
- Zhao, X. et al. LncRNA HOXA11-AS drives cisplatin resistance of human LUAD cells via modulating miR-454-3p/Stat3. *Cancer Sci.* **109**, 3068–3079 (2018).
- Xiong, D. D. et al. The LncRNA NEAT1 Accelerates Lung Adenocarcinoma Deterioration and Binds to Mir-193a-3p as a Competitive Endogenous RNA. *Cell. Physiol. Biochem.* **48**, 905–918 (2018).
- Wang, S. J., Wang, H., Zhao, C. D. & Li, R. Long noncoding RNA LINC01426 promotes glioma progression through PI3K/AKT signaling pathway and serves as a prognostic biomarker. *Eur. Rev. Med. Pharmacol. Sci.* **22**, 6358–6368 (2018).
- Li, J., Wang, J., Chen, Y., Yang, L. & Chen, S. A prognostic 4-gene expression signature for squamous cell lung carcinoma. *J. Cell. Physiol.* **232**, 3702–3713 (2017).
- Liu, L. P. & Gong, Y. B. LncRNA-TCL6 promotes early abortion and inhibits placenta implantation via the EGFR pathway. *Eur. Rev. Med. Pharmacol. Sci.* **22**, 7105–7112 (2018).
- Guo, L. et al. LncRNA ASAP1-IT1 positively modulates the development of cholangiocarcinoma via hedgehog signaling pathway. *Biomed. Pharmacother.* **103**, 167–173 (2018).
- Wang, F. et al. Upregulated lncRNA-UCA1 contributes to progression of hepatocellular carcinoma through inhibition of miR-216b and activation of FGFR1/ERK signaling pathway. *Oncotarget* **6**, 7899–7917 (2015).
- Gao, R., Zhang, R., Zhang, C., Liang, Y. & Tang, W. LncRNA LOXL1-AS1 promotes the proliferation and metastasis of medulloblastoma by activating the PI3K/AKT pathway. *Anal. Cell. Pathol.* **2018**, 9275685 (2018).
- Ming, J. et al. Aspirin inhibits the SHH/GLI1 signaling pathway and sensitizes malignant glioma cells to temozolomide therapy. *Aging* **9**, 1233–1247 (2017).
- Xiao, H. et al. USP22 acts as an oncogene by regulating the stability of cyclooxygenase-2 in non-small cell lung cancer. *Biochem. Biophys. Res. Commun.* **460**, 703–708 (2015).
- Zhang, H. et al. USP22 promotes resistance to EGFR-TKIs by preventing ubiquitination-mediated EGFR degradation in EGFR-mutant lung adenocarcinoma. *Cancer Lett.* **433**, 186–198 (2018).
- Zhou, A. et al. Nuclear GSK3beta promotes tumorigenesis by phosphorylating KDM1A and inducing its deubiquitylation by USP22. *Nat. Cell Biol.* **18**, 954–966 (2016).
- Liu, A. N., Qu, H. J., Yu, C. Y. & Sun, P. Knockdown of LINC01614 inhibits lung adenocarcinoma cell progression by up-regulating miR-217 and down-regulating FOXP1. *J. Cell. Mol. Med.* **22**, 4034–4044 (2018).
- Ge, X. et al. Long noncoding RNA CAR10 promotes lung adenocarcinoma metastasis via miR-203/30/SNAI axis. *Oncogene* **38**, 3061–3076 (2019).
- Zhang, X., Chi, Q. & Zhao, Z. Up-regulation of long non-coding RNA SPRY4-IT1 promotes tumor cell migration and invasion in lung adenocarcinoma. *Oncotarget* **8**, 51058–51065 (2017).
- Wei, C. et al. LPCAT1 promotes brain metastasis of lung adenocarcinoma by up-regulating PI3K/AKT/MYC pathway. *J. Exp. Clin. Cancer Res.* **38**, 95 (2019).
- Wang, Y. et al. Neuregulin1 acts as a suppressor in human lung adenocarcinoma via AKT and ERK1/2 pathway. *J. Thorac. Dis.* **10**, 3166–3179 (2018).
- Zhang, L. et al. FLOT1 promotes tumor development, induces epithelial-mesenchymal transition, and modulates the cell cycle by regulating the Erk/Akt signaling pathway in lung adenocarcinoma. *Thorac. Cancer* **10**, 909–917 (2019).
- Wu, D. et al. Stable knockdown of protein kinase CK2-alpha (CK2alpha) inhibits migration and invasion and induces inactivation of hedgehog signaling pathway in hepatocellular carcinoma Hep G2 cells. *Acta Histochem.* **116**, 1501–1508 (2014).
- Amarante, M. K., Vitiello, G. A. F., Rosa, M. H., Mancilla, I. A. & Watanabe, M. A. E. Potential use of CXCL12/CXCR4 and sonic hedgehog pathways as therapeutic targets in medulloblastoma. *Acta Oncol.* **57**, 1134–1142 (2018).
- Jiang, K. et al. Fms related tyrosine kinase 1 (Flt1) functions as an oncogene and regulates glioblastoma cell metastasis by regulating sonic hedgehog signaling. *Am. J. Cancer Res.* **7**, 1164–1176 (2017).
- Hu, W. G., Liu, T., Xiong, J. X. & Wang, C. Y. Blockade of sonic hedgehog signal pathway enhances antiproliferative effect of EGFR inhibitor in pancreatic cancer cells. *Acta Pharmacologica Sin.* **28**, 1224–1230 (2007).
- Zhao, H. et al. MiR-101 targets USP22 to inhibit the tumorigenesis of papillary thyroid carcinoma. *Am. J. Cancer Res.* **6**, 2575–2586 (2016).
- Ma, Y. X., Zhang, H., Li, X. H. & Liu, Y. H. MiR-30e-5p inhibits proliferation and metastasis of nasopharyngeal carcinoma cells by target-ing USP22. *Eur. Rev. Med. Pharmacol. Sci.* **22**, 6342–6349 (2018).
- Zhou, D. et al. USP22 down-regulation facilitates human retinoblastoma cell aging and apoptosis via inhibiting TERT/P53 pathway. *Eur. Rev. Med. Pharmacol. Sci.* **21**, 2785–2792 (2017).
- Popovic, D., Vucic, D. & Dikic, I. Ubiquitination in disease pathogenesis and treatment. *Nat. Med.* **20**, 1242–1253 (2014).
- Ni, W. et al. A novel lncRNA uc134 represses hepatocellular carcinoma progression by inhibiting CUL4A-mediated ubiquitination of LATS1. *J. Hematol. Oncol.* **10**, 91 (2017).
- Jin, L. et al. Long noncoding RNA MEG3 regulates LATS2 by promoting the ubiquitination of EZH2 and inhibits proliferation and invasion in gallbladder cancer. *Cell Death Dis.* **9**, 1017 (2018).